NATURAL SCIENCE REVIEW 1 5 (2024)
nsr.jinr.int

Search for $K_{S,L}$ oscillations and invisible decays into the dark sector at NA64

S. N. Gninenko[1,2], N. V. Krasnikov*[1,2], and V. A. Matveev[1,2]

[1] *Institute for Nuclear Research of the Russian Academy of Sciences, Moscow, Russia*
[2] *Joint Institute for Nuclear Research, Dubna, Russia*

Abstract

The decays $K_{S,L} \to invisible$ have never been experimentally tested. In the Standard Model (SM), their branching ratios for the decay into two neutrinos are predicted to be extremely small, $\mathrm{Br}\,(K_{S,L} \to \nu\bar{\nu}) \lesssim 10^{-16}$. We consider several natural extensions of the SM, such as two-Higgs-doublet (2HDM), 2HDM and light scalar, and dark mirror sector models, that allow one to enhance the $\mathrm{Br}\,(K_{S,L} \to invisible)$ up to a measurable level. We briefly discuss the possible search for $K_{S,L} \to invisible$ decays and $K_{S,L}$ oscillations into the dark sector at the NA64 experiment at CERN with the sensitivity to $\mathrm{Br}\,(K_{S,L} \to invisible) \lesssim 10^{-7}$–$10^{-5}$.

Keywords: kaon physics, search for kaon oscillations, search for new physics at fixed target experiments

1. Introduction

Experimental studies of invisible decays, i.e., particle transitions to an experimentally unobservable final state, played an important role both in the development of the Standard Model (SM) and in testing its extensions [1]. It is worth remembering the precision measurements of the $Z \to invisible$ decay rate at LEP for the determination of the number of lepton families in the SM. In recent years, experiments on invisible particle decays have received considerable attention. Motivated by various models of physics beyond the SM, see, e.g., [2–14] and references therein, these experiments include searches for invisible decays of π^0 mesons at E949 [15] and NA62 [16], η and η' mesons at BES [17] and NA64 [18], heavy B-meson decays at Belle [19], BaBAR [20], and BES [21], and invisible decays of the $\Upsilon(1S)$ resonance at CLEO [22], baryonic number violation with nucleon disappearance at SNO [23], BOREXINO [24], and KamLAND [25], see also [26], electric charge-nonconserving electron decays $e^- \to invisible$ [27], neutron–mirror-neutron oscillations at PSI [28, 29] and the ILL reactor [30], and the disappearance of neutrons into another brane world [31]. One could also mention experiments looking for extra dimensions and dark mirror matter through the invisible decays of positronium [32–34], and plans for new experiments to search for muonium annihilation into two neutrinos, $\mu^+ e^- \to \nu\bar{\nu}$ [35], and electric charge nonconservation in the muon decay $\mu^+ \to invisible$ [36].

*Corresponding author e-mail address: Nikolai.Krasnikov@cern.ch

Received: 09 December 2024; Revised: 16 December 2024; Accepted: 17 December 2024; Published: 23 December 2024

The aim of this paper is to discuss an experiment with the NA64 detector at CERN modified for the sensitive search for $K_{S,L} \to invisible$ decays. The rest of the paper is organized as follows. In Sections 2, 3 and 4, we briefly review the motivations to perform the search, and several natural extensions of the SM, such as two-Higgs-doublet (2HDM), 2HDM and light scalar, and mirror dark sector models, which allow one to enhance the $\mathrm{Br}\,(K_{S,L} \to invisible)$ up to a measurable level. In Section 5 we discuss the search method and the NA64 setup modified for the searching for $K_{S,L} \to invisible$ decays, and K^0–dark K^0 oscillations. The background sources and the expected sensitivity are also discussed. Section 6 contains concluding remarks.

2. Motivations

The decays $K_{S,L} \to invisible$ have never been experimentally tested despite the extensive search program of new physics in kaon decays [1]. The first bound on $\mathrm{Br}\,(K_{S,L} \to invisible) \lesssim 10^{-4}$–$10^{-3}$ has been set assuming validity of unitarity in the K^0 sector from the existing experimental data [4]. From the experimental viewpoint, the K mesons themselves have brought to the SM so many surprises that all their still unknown properties deserve to be carefully studied. Since long ago it was recognized that $K_{S,L} \to invisible$ decays "would be interesting to explore, but its detection looks essentially impossible. New ingenious experimental ideas are required" [37].

One of the approaches proposed not long ago in [4] is based on the idea to use charge-exchange reaction as a source of well-tagged neutral mesons. In this process, the $K_{S,L} \to invisible$ events would exhibit themselves via a striking signature — the complete disappearance of the incoming beam energy in the detector. The first results on the search for the $\eta, \eta' \to invisible$ decay modes recently obtained by the NA64 Collaboration at the CERN SPS [18] provide proof of concept and suggest the overall future direction for performing such kinds of experiments with this approach.

2.1. General considerations

The $K_{S,L} \to invisible$ decays are complementary to the $K^+ \to \pi^+ + invisible$ and $K_L \to \pi^0 + invisible$ decays, whose branching ratios in the SM are predicted to be [39]

$$\mathrm{Br}\,(K_L \to \pi^0 \nu\bar{\nu}) = (2.6 \pm 0.4) \cdot 10^{-11}\,, \tag{2.1}$$

$$\mathrm{Br}\,(K^+ \to \pi^+ \nu\bar{\nu}) = (8.5 \pm 0.7) \cdot 10^{-11}\,, \tag{2.2}$$

with the invisible final state represented by neutrino pairs. A powerful comparison between experiment and theory is possible due to the accuracy of both the measurements and the SM calculations of these observables. A discrepancy would signal the presence of physics beyond the Standard Model (BSM), making the precision study of these decays an effective probe to search for it, see, e.g., [39–44].

On the contrary, the searching for invisible decays of the K_S and K_L, and other pseudoscalar mesons (M^0), such as π^0, η, η', is particularly advantageous because in the SM the branching fraction of their decay into a neutrino–antineutrino pair, $\mathrm{Br}\,(M^0 \to \nu\overline{\nu})$, is predicted to be extremely small [37]. For massless neutrinos, this transition is forbidden kinematically by angular momentum conservation. Indeed, in the M^0 rest frame the neutrinos produced in the decay fly away in opposite directions along the same line. Since the neutrinos and antineutrinos are massless, the projection of the sum of their spins on this line equals ± 1. The projections of the orbital angular momentum of the neutrino on this line are equal to zero. Since in the initial state we have a scalar, the process is forbidden. For the case of massive neutrinos, one of them is forced to have the "wrong" helicity resulting in the suppression of $\mathrm{Br}\,(M^0 \to \nu\overline{\nu})$ by a factor proportional to the neutrino mass squared,

$$\mathrm{Br}\,(M^0 \to \nu\overline{\nu}) \sim \frac{m_\nu^2}{m_{M^0}^2} \lesssim 10^{-16}, \tag{2.3}$$

for $m_\nu \lesssim 10$ eV and $m_{M^0} \simeq m_K \simeq 0.5$ GeV [1]. In the SM the helicity suppression can be overcome for the four-neutrino final state; however, in this case, $\mathrm{Br}\,(M^0 \to \nu\overline{\nu}\nu\overline{\nu}) \lesssim 10^{-18}$ [38]. Therefore, differently form the decays (2.1), (2.2), observation of the $M^0 \to$ *invisible* decay for any of M^0 mesons would unambiguously signal the presence of BSM physics.

2.2. The Bell–Steinberger unitary relation

Another important reason to look for $K_S, K_L \to$ *invisible* decays is related to additional tests of the K^0–$\overline{K}^0$ system using the Bell–Steinberger relation [45]. This relation, obtained by using the unitarity condition, connects CP and CPT violation in the mass matrix of the kaon system, i.e., parameters describing T and CPT noninvariance, to CP and CPT violation in all decay channels of neutral kaons, see, e.g., [46–50]. The CPT appears to be an exact symmetry of nature, while C, P and T are known to be violated. Hence, testing the validity of the CPT invariance probes the basis of the SM. The Bell–Steinberger relation remains one of the most sensitive tests of CPT symmetry, resulting, for example, in the impressive sensitivity of $-5.3 \cdot 10^{-19}$ GeV $< m_{K^0} - m_{\overline{K}^0} < 6.3 \cdot 10^{-19}$ GeV at 95% C.L. for the neural kaon mass difference [51, 52]. However, the question of how much the invisible decays of K_S or K_L can influence the precision of the Bell–Steinberger analysis still remains open [53]. This makes the future searches for these decay modes very interesting and complementary to the study of other $K_{S,L}$ decays.

Briefly, within the Wigner–Weisskopf approximation, the time evolution of the neutral kaon system is described by [51]

$$i\frac{d\Phi(t)}{dt} = H\Phi(t) = \Big(M - \frac{i}{2}\Gamma\Big)\Phi(t), \tag{2.4}$$

where M and Γ are 2×2 Hermitian matrices, which are time-independent, and $\Phi(t)$ is a two-component state vector in the K^0–$\overline{K}^0$ space. Denoting by m_{ij} and Γ_{ij} the elements of M and Γ in the K^0–$\overline{K}^0$basis, CPT invariance implies

$$\begin{gathered} m_{11} = m_{22} \quad (\text{or} \quad m_{K^0} = m_{\overline{K}^0}) \quad \text{and} \\ \Gamma_{11} = \Gamma_{22} \quad \big(\text{or} \quad \Gamma_{K^0} = \Gamma_{\overline{K}^0}\big)\,. \end{gathered} \tag{2.5}$$

The eigenstates of Eq. (2.4) can be written as

$$\begin{aligned} K_{S,L} = \frac{1}{\sqrt{2(1+|\epsilon_{S,L}|^2)}}\Big((1+\epsilon_{S,L})K^0 \pm \\ \pm\,(1-\epsilon_{S,L})\overline{K}^0\Big) \end{aligned} \tag{2.6}$$

with

$$\epsilon_{S,L} = \frac{1}{m_L - m_S + i(\Gamma_S - \Gamma_L)/2}\Big[-i\,\mathrm{Im}\,(m_{12}) - \\ -\frac{1}{2}\mathrm{Im}\,(\Gamma_{12}) \pm \frac{1}{2}(m_{\overline{K}^0} - m_{K^0} - \frac{i}{2}(\Gamma_{\overline{K}^0} - \Gamma_{K^0})\Big] \equiv \epsilon \pm \delta. \tag{2.7}$$

The unitarity condition allows us to express the four elements of Γ in terms of appropriate combinations of the kaon decay amplitudes A_i:

$$\Gamma_{ij} = \sum_f A_i(f)A_j^*(f), \quad i,j = 1,2 = K^0, \overline{K}^0, \tag{2.8}$$

where the sum is over all the accessible final states:

$$\left(\frac{\Gamma_S + \Gamma_L}{\Gamma_S - \Gamma_L} + i\tan\phi_{SW}\right)\left(\frac{\mathrm{Re}\,(\epsilon)}{1+|\epsilon|^2} - i\,\mathrm{Im}\,(\delta)\right) = \\ = \frac{1}{\Gamma_S - \Gamma_L}\sum_F A_L(f)A_S^*(f), \tag{2.9}$$

where $\phi_{SW} = \arctan[2(\mathrm{m_L} - \mathrm{m_S})/(\Gamma_\mathrm{S} - \Gamma_\mathrm{L})]$. One can see that the Bell–Steinberger relation (2.9) relates a possible violation of CPT invariance ($m_{K^0} = m_{\overline{K}^0}$ and/or $\Gamma_{K^0} = \Gamma_{\overline{K}^0}$) in the $K^0 - \overline{K}^0$ system to the observable CP-violating interference of K_S and K_L decays into the same final state f. If CPT invariance is not violated, then $\mathrm{Im}\,(\delta) = 0$. We stress that any evidence for $\mathrm{Im}\,(\delta) \neq 0$ resulting from this relation can only manifest the violation of CPT or unitarity [47].

Generally, the advantage of the neutral kaon system is attributed to the fact that only a few (hadronic) decay modes give significant contributions to the rhs of Eq. (2.9). However, what are the contributions from $K_{S,L} \to invisible$ decay modes and how much the errors on $\mathrm{Re}\,(\epsilon)$ and $\mathrm{Im}\,(\delta)$ would increase if these modes have maximal CP violation are still open questions, see, e.g., [53], which have to be answered experimentally.

Using the results of the most precise measurements of the branching fractions of the visible K_S, K_L decay modes from Particle Data Group (PDG) [1], the estimate of the allowed extra contribution of $K_S, K_L \to invisible$ decays to the total decay rate of K_S and K_L result, respectively, in

$$\mathrm{Br}\,(K_S \to invisible) < 1.1 \cdot 10^{-4} \text{ (95\% C.L.)}, \tag{2.10}$$

and

$$\mathrm{Br}\,(K_L \to invisible) < 6.3 \cdot 10^{-4} \text{ (95\% C.L.)}, \tag{2.11}$$

which would be interesting to check, see [4] for more discussions.

3. Models with $K_{S,L} \to invisible$ decays

Being motivated by the above considerations, we discuss in this section several natural extensions of the SM predicting the existence of invisible K_S, K_L decays [5, 6]. We show that, taking into account the most stringent constraints from the measured $K^+ \to \pi^+ + invisible$ decay rate, the decay $K_{S,L} \to invisible$ could occur at the level of $\mathrm{Br}\,(K_{S,L} \to invisible) \simeq 10^{-8}$–$10^{-6}$. The main feature of the considered models, which leads to the enhanced $\mathrm{Br}\,(K_{S,L} \to invisible)$ compared to those from Eqs. (2.1), (2.2), is that they allow one to avoid the helicity suppression factor $\left(\frac{m_\nu}{m_{K_L}}\right)^2$ of the SM, while profiting from its larger phase-space due to the decay into two light weakly interacting particles. In addition, there might be the case when $K_{S,L} \to invisible$ could still be kinematically allowed, while $K^+ \to \pi^+ + invisible$ is forbidden.

3.1. The model with additional Higgs isodoublet

Probably, the simplest model predicting K_S, K_L invisible decays is the model with additional Higgs isodoublet $H_2 = (H_2^+,\ H_2^0)$ [5]. The additional Higgs isodoublet with zero vacuum expectation value $\langle H_2 \rangle = 0$ interacts with quarks generations, namely,

$$L_{H_2,\text{quarks}} = -h_{ij}\bar{Q}_{Li}H_2 d_{Rj} + \text{h.c.}, \tag{3.1}$$

where $d_{R1} = d_R$, $d_{R2} = s_R$, $d_{R3} = b_R$ and $Q_{L1} = (u,d)_L$, $Q_{L2} = (c,s)_L$, $Q_{L3} = (t,b)_L$. We discuss the physics of K mesons, so we omit the effects related with the third generations of quarks. In general, for $h_{12}h_{21}^* \neq 0$ the interaction (3.1) leads to flavour violating $\Delta S = 2$ currents. The measured $K_L - K_S$ mass difference and the CP-violation parameter ϵ_K strongly restricts (as a review, see, for example, [54]) the effective $\Delta S = 2$ interaction

$$L_{\Delta S=2} = \frac{1}{\Lambda^2_{\Delta S=2}}\bar{d}_L s_R \bar{d}_R s_L + \text{h.c.}, \tag{3.2}$$

namely [54],

$$|\text{Re}\,(\Lambda_{\Delta S=2}| \geqslant 1.8 \cdot 10^7 \text{ GeV}, \tag{3.3}$$

$$|\text{Im}\,(\Lambda_{\Delta S=2}| \geqslant 3.2 \cdot 10^8 \text{ GeV}. \tag{3.4}$$

For the considered model (3.1), we find that

$$\frac{1}{\Lambda^2_{\Delta S=2}} = \frac{h_{12}h_{21}^*}{M^2_{H_2}}\,. \tag{3.5}$$

We shall assume that h_{12} and h_{21} are real. As a consequence, the Yukawa interaction (3.1) is CP-conserving and the most strongest bound (3.4) on the $\Delta S = 2$ currents is avoided. For CP-conserving interaction, as a consequence of formulae (3.3) and (3.5), the bound on the mass of the second Higgs isodoublet reads

$$M_{H_2} \geqslant 1.8|h_{21}h_{12}|^{1/2} \cdot 10^7 \text{ GeV}. \tag{3.6}$$

In the considered model, the second Higgs isodoublet H_2 also interacts with leptons

$$L_{H_2,\ \text{leptons}} = -h_{Lk}\bar{L}_k\tilde{H}_2\nu_{Rk} + \text{h.c.}, \tag{3.7}$$

where $L_1 = (\nu_{Le},\ e_L)$, $L_2 = (\nu_{L\mu}, \mu_L)$, $L_3 = (\nu_{L\tau}, \tau_L)$, $\tilde{H}_2 = (-(H_2^0)^*, (H_2^+)^*)$ and ν_{Rk} ($k = 1,2,3$) are right-handed neutrinos. We assume that the right-handed neutrino masses $m_{\nu_{Rk}}$ are much smaller than the K^0-meson mass. As a consequence of interactions (3.1) and (3.7), the K_L, K_S mesons will decay invisibly into $K_L, K_S \to \nu_{Lk}\bar{\nu}_{Rk},\ \nu_{Rk}\bar{\nu}_{Lk}$ with the decay width

$$\Gamma(K_L(K_S) \to \nu_{Lk}\bar{\nu}_{Rk},\ \nu_{Rk}\bar{\nu}_{Lk}) = \frac{M^5_{K_L}}{16\pi M_X^4}\left(\frac{F_K}{2(m_d+m_s)}\right)^2 K\left(\frac{m^2_{R1}}{M^2_{K_L}}\right), \tag{3.8}$$

where

$$\frac{1}{M_X^4} = \frac{|(h_{12}+(-)h_{21})|^2 \cdot (|h_{L1}|^2 + |h_{L2}|^2 + |h_{L3}|^2)}{M^4_{H_2}} \tag{3.9}$$

and $K(x) = (1-x)^2$ for Majorana neutrino with a mass m_{R1} and massless neutrino ν_{L1}[1]. Here $F_K \approx 160$ MeV is kaon lepton decay constant and m_d, m_s are the masses of d and s quarks.

[1] In formula (3.9) the sign "+" corresponds to the K_L decay and the sign "−" corresponds to the K_S decay.

In our estimates we take $(m_s + m_d)(2\text{ GeV}) = 100$ MeV and $\Gamma_{\text{tot}}(K_L) = 1.29 \cdot 10^{-17}$ GeV, $\Gamma_{\text{tot}}(K_S) = 7.35 \cdot 10^{-15}$ GeV. Using formula (3.8), we find that for $\text{Br}\,(K_L \to \nu_{Ll}\bar{\nu}_{Rk},\, \nu_{Rk}\bar{\nu}_{Lk}) = 10^{-6}$ we can test the values of M_X up to

$$M_X \leqslant 0.74 \cdot 10^5 \text{ GeV } (1.5 \cdot 10^4 \text{ GeV}) \tag{3.10}$$

for $K_L(K_S)$ mesons.

It should be noted that the bound (3.6) strongly restricts, but not excludes, phenomenologically interesting values of M_X and invisible neutral K-meson decays with the branching at the level of $O(10^{-6})$. For instance, for $h_{12} = h_{21} = 2 \cdot 10^{-5}$ $(2 \cdot 10^{-4})$, $h_{L1} = h_{L2} = h_{L3} = 1$ and $M_{H_2} = 400$ (4000) GeV, we find that $\Lambda_{\Delta S=2} = 2 \cdot 10^7$ GeV and $\text{Br}\,(K_L \to \nu_k\bar{\nu}_k) = 5.7 \cdot 10^{-6}$ $(5.7 \cdot 10^{-8})$. For the case $h_{12} = 0$ or $h_{21} = 0$, the bound (3.6) dissapears.

3.2. The model with additional scalar isodoublet and isosinglet

In this subsection we consider the modification of the previous model. Namely, in addition to the second Higgs isodoublet H_2, we add neutral scalar isodoublet ϕ with the interaction

$$L_{H_2 H\phi\phi} = -\lambda H_2^+ H\phi\phi + \text{h.c.} \tag{3.11}$$

After electroweak symmetry breaking, the effective trilinear term

$$L_{H_2\phi\phi} = -\lambda\langle H\rangle(H_2^0 + (H_2^0)^*)\phi\phi \tag{3.12}$$

becomes responsible for the interaction of ϕ particles with quarks. Here $\langle H\rangle = 176$ GeV. The effective Lagrangian looks like

$$L_{\text{eff}} = \frac{\lambda\langle H\rangle}{M_{H_2}^2}[h_{12}\bar{d}_L s_R + h_{21}\bar{s}_L d_R + \text{h.c.}]\phi^2. \tag{3.13}$$

The K_L decay width $K_L \to \phi\phi$ is of the form

$$\Gamma(K_L \to \phi\phi) = \left(\frac{\lambda\langle H\rangle}{M_{H_2}^2}\right)^2 |h_{12} + h_{21} - h_{12}^* - h_{21}^*|^2 \frac{M_{K_L}^3}{64\pi}\left(\frac{F_K}{2(m_d + m_s)}\right)^2 K\left(\frac{m_\phi^2}{M_{K_L}^2}\right), \tag{3.14}$$

where $K(x) = (1 - 4x)^{1/2}$. The formula for K_S decay width has a similar form:

$$\Gamma(K_L \to \phi\phi) = \left(\frac{\lambda\langle H\rangle}{M_{H_2}^2}\right)^2 |h_{12} - h_{21} + h_{12}^* - h_{21}^*|^2 \frac{M_{K_L}^3}{64\pi}\left(\frac{F_K}{2(m_d + m_s)}\right)^2 K\left(\frac{m_\phi^2}{M_{K_L}^2}\right), \tag{3.15}$$

Note that the model proposed in [6] also predicts the existence of K_L, K_S invisible decays. The peculiarity of the model [6] is the use of nonrenormalizable Lagrangian

$$L_{\phi,\text{ quarks}} = -h_{ij}\bar{Q}_{Li}Hq_{Rj}\phi + \text{h.c.} \tag{3.16}$$

Here, ϕ is a neutral $(\phi^* = \phi)$ scalar field with a mass m_ϕ, and $H = (H^+, H^0)$ is the SM Higgs isodoublet. It is also assumed that the field ϕ couples with right-handed neutrino (dark matter). The corresponding formulae for K_L, K_S invisible decay widths and the bounds on the h_{ij} coupling constants are contained in [6], and they are similar to formulae (3.6), (3.8).

4. Oscillations of K_S, K_L into the dark mirror sector

Today the origin of dark matter (DM) in the Universe is still a great puzzle, see, e.g., [55, 56]. The possible existence of the dark mirror sector part of which is mirror DM with particle and interaction content identical to a mirror copy of the SM has still received significant attention, as the DM could be explained by the existing of the mirror baryons [57–60]. If the dark mirror sector exists, the mixing between the SM neutral states, such as positronium (Ps) − mirror-positronium (Ps^M) [61], neutron (n) − mirror-neutron (n^M) [62], and K^0–mirror-K^{0M} [63] are possible, resulting in oscillations of SM states into the corresponding mirror ons. The searches for this effect have been performed for the Ps−Ps^M [34] and n−n^M [28–30] oscillations, but not for the K^0−K^{0M} system yet.

Probably, the simplest model predicting the K^0−K^{0M} oscillations is the following [5]. In the SM and mirror SM models, two additional Higgs isodoublets H_2 and H_2^M are introduced and the interaction of $H_2(H_2^M)$ isodoublets with quarks (mirror quarks) is of the form (3.1). The interaction of H_2, H_2^M isodoublets with the standard H and H^M isodoublets takes the form

$$L_{H_2 H_2^M} = -\lambda_M (H_2^+ H)(H^+ H_2^M) + \mathrm{h.c.} \tag{4.1}$$

After electroweak symmetry breaking, we find that the effective interaction

$$L_{\mathrm{eff,mix}} = -\lambda_M (\langle H\rangle)^2 (H_2^0)^* (H_2^{0M}) + \mathrm{h.c.} \tag{4.2}$$

is responsible for the mixing of K^0 and K^{0M} mesons. Namely, as a consequence of nonzero mixing (4.2), the four-fermion interaction

$$L_{\mathrm{4ferm,mix}} = \frac{1}{M_{\mathrm{eff}}^2}[(h_{ij}\bar{d}_{Li}d_{Rj})\cdot(h_{ij}\bar{d}_{Li}^M d_{Rj}^M)^* + [(h_{ij}\bar{d}_{Li}d_{Rj})^*\cdot(h_{ij}\bar{d}_{Li}^M d_{Rj}^M)] \tag{4.3}$$

leads to the oscillations between K^0 and K^{0M} mesons. Here,

$$\frac{1}{M_{\mathrm{eff}}^2} = \frac{(\lambda_M \langle H\rangle)^2}{M_{H_2}^4}. \tag{4.4}$$

As an example, consider the case of K_L−K_L^M oscillations. The mixing between K_L and K_L^M mesons is described by the effective Hamiltonian

$$H_{\mathrm{mix}} = \delta K_L K_L^M. \tag{4.5}$$

The states $K_\pm = \frac{1}{\sqrt{2}}(K_L \pm K_L^M)$ have the masses $m_\pm = (m_{K_L} \pm \frac{\delta}{2})$. An ordinary K_L produced in strong interactions would oscillate into mirror K_L^M state with the probability determined by

$$P(K_L \to K_L^M|t) = |\langle K_L^M(t)|K_L(t=0)\rangle|^2 = \frac{1}{4}|1-\exp(-i\delta t)|^2 \exp(-\Gamma_{K_L} t). \tag{4.6}$$

The full probability at the time $t_0 \geqslant t \geqslant 0$ is given by the formula

$$P_{\mathrm{int}}(K_L \to K_L^M|t \leqslant t_0) \equiv \int_0^{t_0} dt\, |\langle K_L^M(t)|K_L(t=0)|\rangle^2, \tag{4.7}$$

resulting in

$$\begin{aligned} P_{\mathrm{int}}(K_L \to K_L^M|t \leqslant t_0) &= \frac{\delta^2}{2\Gamma_{K_L}(\Gamma_{K_L}^2+\delta^2)} \times \\ \times(1-\exp(-\Gamma_{K_L}t_0)) &+ \frac{\Gamma_{K_L}(\cos(\delta t_0)-1) - \Delta\sin(\delta t_0)}{2(\Gamma_{K_L}^2+\delta^2)}\exp(-\Gamma_{K_L}t_0)). \end{aligned} \tag{4.8}$$

The integration over time gives the full probability for the $K_L \to K_L^M$ conversion:

$$P_{\rm int}(K_L \to K_L^M | t \leqslant \infty) = \frac{\delta^2}{2\Gamma_{K_L}(\Gamma_{K_L}^2 + \delta^2)}. \tag{4.9}$$

The relative probability for K_L to oscillate into K_L^M state at the time $t_0 \geqslant t \geqslant 0$ is determined by the formula

$$P_{\rm rel}(K_L \to K_L^M | t \leqslant t_0) \equiv \frac{\int_0^{t_0} dt\, |\langle K_L^M(t)|K_L(t=0)\rangle|^2}{\int_0^{t_0} dt\, |\langle K_L(t)|K_L(t=0)\rangle|^2}. \tag{4.10}$$

In particular,

$$P_{\rm rel}(K_L \to K_L^M | t \leqslant \infty) = \frac{\delta^2}{2(\Gamma_{K_L}^2 + \delta^2)}, \tag{4.11}$$

assuming $\Gamma_{K_L} \gg \delta$.

Note that all previous formulae were derived for K mesons in the rest frame. For kaons moving with the momentum $\vec{p}$, we must have the replacements $m_\pm = m \pm \frac{\delta}{2} \to \tilde{m}_\pm = m \pm \frac{\delta}{2} - i\frac{\Gamma_{K_L}}{2}$ in formulae $E_\pm = \sqrt{\vec{p}^{\,2} + m_\pm^2}$ for kaon energies. For $m \gg \delta,\ \Gamma$ we have to perform the replacements $\Gamma \to \Gamma \cdot \frac{m}{\sqrt{\vec{p}^{\,2}+m^2}}$, $\delta \to \delta \cdot \frac{m}{\sqrt{\vec{p}^{\,2}+m^2}}$ in formulae (4.6), (4.9), which take the form

$$P(K_L \to K_L^M | t) = \frac{1}{2}\left(1 - \cos\left(\delta \frac{m}{\sqrt{\vec{p}^{\,2} + m^2}} t\right)\right) \exp\left(-\Gamma_{K_L} \cdot \frac{m}{\sqrt{\vec{p}^{\,2} + m^2}} t\right) \tag{4.12}$$

and

$$P_{\rm int}(K_L \to K_L^M) | t \leqslant \infty) = \frac{\delta^2}{2\Gamma_{K_L}(\Gamma_{K_L}^2 + \delta^2)} \cdot \frac{\vec{p}^{\,2} + m^2}{m^2}, \tag{4.13}$$

respectively.

5. A search for $K_{S,L} \to invisible$ decays and oscillations into dark sector

In this section, we discuss briefly an experiment on searching for $K_{S,L} \to invisible$ decays and $K_{S,L} - K_{S,L}^M$ oscillations within the NA64 experimental program at CERN, see, e.g., [64, 65]. The signature of the latter would be the disappearance of the $K_{S,L}$ from the beam due to their $K_{S,L} \to invisible$ decays in flight into invisible dark final states. Searching for $K_{S,L} \to invisible$ decays is challenging, as it requires a combination of an intense source of K^0s and a well-defined high-purity signature to tag their production. Currently, there is no experimental limits on $K_S, K_L \to invisible$ decay modes, apart from those, see (2.10) and (2.11), obtained assuming that unitarity is the fundamental property of the $K_{S,L}$ decays [4].

5.1. The search method and the experimental setup

The general method for searching for neutral meson $M^0(\pi^0, \eta, \eta', K_S, K_L \ldots) \to invisible$ decays was proposed in [4]. Recently, the NA64 Collaboration at CERN obtained the first proof-of-concept results on the search for $\eta, \eta' \to invisible$ decays based on this method [18], which is briefly described below.

The source of M^0 could be either the quasi-elastic charge-exchange reaction of high-energy kaons on nuclei of an active target

$$\begin{aligned} K^- + A(Z) &\to \overline{K}^0 + n + A(Z-1), \quad \text{or} \\ K^+ + A(Z) &\to K^0 + p + A(Z) \end{aligned} \tag{5.1}$$

or high-energy $\pi^{\pm}$-induced reactions

$$\begin{aligned} &\pi^- + A(Z) \to \eta, \eta', \ldots + n + A(Z-1), \\ &\pi^- + A(Z) \to K^0 + \Lambda + A(Z-1), \\ &\pi^+ + A(Z) \to K^0 + \Sigma^+ + A(Z). \end{aligned} \tag{5.2}$$

The reactions with $\pi^{\pm}$ are more interesting for the $K_{S,L} \to invisible$ search compared to (5.1), due to the significantly higher intensity of $\pi^{\pm}$ beams and comparable cross sections of the K^0 production in (5.1) and (5.2). In these quasi-elastic processes, e.g., the neutral kaon is emitted mainly in the forward direction with the beam momentum and the recoil nucleon/nuclei carries/carry away a small fraction of the beam energy. The term "quasi-elastic reaction" means that, unlike elastic reactions of charge exchange with the proton (neutron), the transition can occur for the target nucleus as a whole into an excited state followed by its fragmentation. Since the binding energy in the nucleus is a few MeV/nucleon, the velocity $v \sim q$/mass of the daughter particles, where $q \lesssim 0.05$ GeV/c is the momentum transfer, is on average small. At high initial energies, the nucleus does not have time to collapse during the interaction (the characteristic transverse distances is $l \simeq 1/q$). After the collision, the nucleus disintegrates into fragments, which are absorbed into the target. Hence the experimental signature of the M^0 production in (5.1) or (5.2) is an event with *full disappearance of the beam energy*. The decay $K_S, K_L \to invisible$ is expected to be a very rare event that occurs with a much smaller frequency than the $K_{S,L} \to invisible$ production rate. Hence, its observation presents a challenge for the design and performance of the detector. However, despite a relatively small $K_{S,L} \to invisible$ production rate, the signature of the signal event is very powerful, allowing a strong background rejection.

The detector designed to search for the $K_S, K_L \to invisible$ decays is schematically shown in Figure 1 and is complementary to the one proposed for the NA64 search for invisible decays of dark photons at CERN [66, 67]. The experiment employs the T9 (or H4) $\pi^{\pm}$ and $K^{\pm}$ beams, which are produced in a target of the CERN PS (SPS) and transported to the detector

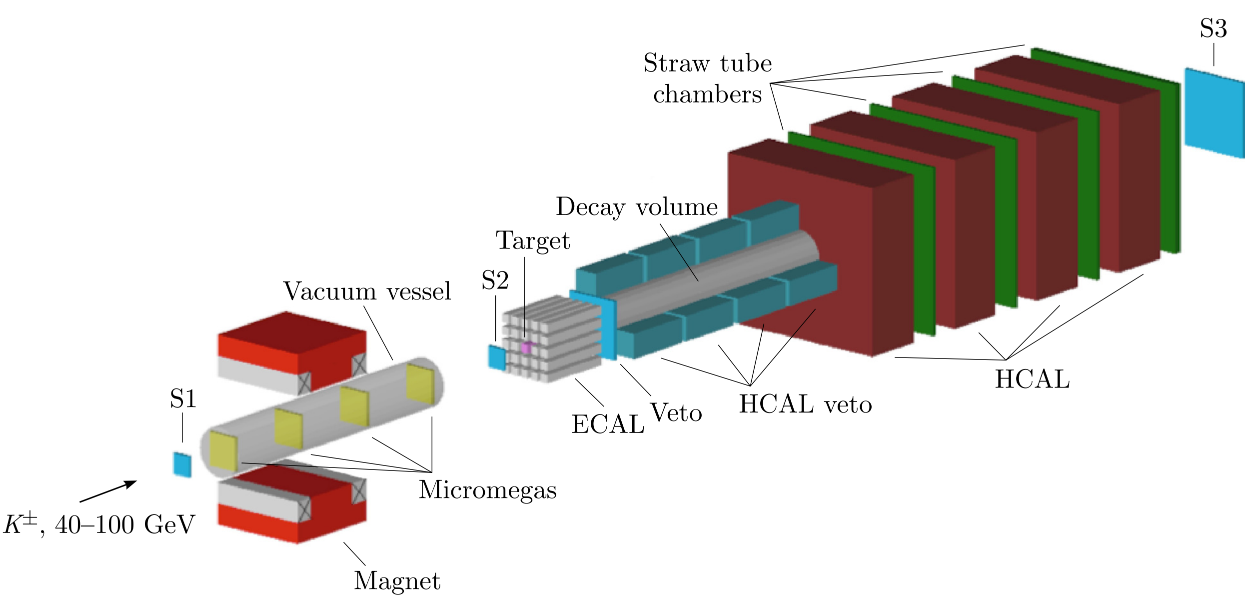

Figure 1. Schematic illustration of the setup to search for the $M^0 \to invisible$ decays and $K_{S,L}-K^M_{S,L}$ oscillations (see text).

by a beamline tuned to a freely adjustable beam momentum around ~ 15 GeV/c (see, for example, [68]). The maximal T9 beam intensity is $\simeq 10^6$ $\pi^\pm$ with the fraction of $K^\pm \sim$ a few percent per PS spill. The typical PS cycle for fixed-target (FT) operation lasts 16.8 s, including two spills of ~ 0.4 s duration. The maximal number of FT cycles is four per minute. The beam has low purity — the admixture of the other charged particles is a few percent. It can be focused onto a spot of the order of a few square centimeters. The incident charged particle is defined by the scintillating counters S1, S2. The momentum of the beam is additionally selected with a momentum spectrometer consisting of a dipole magnet and a low-density tracker, made of a set of Micromegas detectors (MM) or Straw Tube chambers (ST). The setup is a completely hermetic detector allowing for measuring accurately the full energy deposition from reactions (5.1), (5.2). It is equipped with an active target T made of a segmented scintillator counters, surrounded by a high-efficiency electromagnetic calorimeter (ECAL) serving as a veto against photons and other secondaries emitted from the target at large angles and mimicking reactions (5.1), (5.2), high-efficiency forward veto counter (Veto), a decay vacuum volume (DV) surrounded by a thick veto hadronic calorimeter modules (HCAL veto), followed by a massive, hermetic hadronic calorimeter (HCAL) located at the end of the setup and separated by a large-size Straw Tube chambers. For searches at low energies, Cherenkov counters to tag the incoming hadron and enhance it identification (ID) can be used.

Reactions (5.1) and (5.2) occur practically uniformly over the target length. The distribution of the primary kaon (pion) energy deposited in the target can be used as a signature of the M^0 production, see Subsection 5.2, and to determine the position of the interaction vertex along the beam direction. The produced K^0 — composed of equal portions of K_S and K_L — either decays quickly in the target T or penetrates the veto system without interactions, and either decays in flight in the DV or interacts in the HCAL. If the K_S and K_L decay invisibly, it is assumed that the final-state particles in this case also penetrate the rest of the detector without prompt decay into ordinary particles, which could deposit energy in the HCAL. The full HCAL calorimetric system, surrounding the decay volume, is designed to detect with high efficiency the energy deposited by secondaries from the primary interactions $K^\pm A \to$ *anything* in the target. In order to suppress background due to the detection inefficiency, the detector must be longitudinally completely hermetic. To enhance detector hermeticity, the HCAL calorimeter has a total thickness of $\simeq 28\lambda_{\rm int}$ (nuclear interaction lengths) and has to have high light yield to minimize background from the statistical fluctuations of the photoelectrons.

The setup configuration shown in Figure 1 also allows one to search for $K_{S,L}$–$K^M_{S,L}$ oscillations. An ordinary K_L produced in strong interactions, e.g., (5.2), would oscillate into mirror $K^M_{S,L}$ state with the probability determined by Eq. (4.12). The occurrence of the $K_{S,L}$–$K^M_{S,L}$ transition would exhibit itself as the disappearance of the $K_{S,L}$'s from the beam, i.e., as the $K_{S,L} \to$ *invisible* decay, with the rate given by Eq. (4.13) as a function of the $K_{S,L}$ flight-time t, assuming $\tau_S < t < \tau_L$. The occurrence of $K_S, K_L \to$ *invisible* decays produced in $K^\pm$ interactions would appear as an excess of events with a signal in the T, see Figure 1 and zero energy deposition in the rest of the detector (i.e., above that expected from the background sources).

5.2. The K^0 tagging system

To reduce the counting rate and ensure the effective K^0 selection, one could use a system surrounding the T target for the efficient tagging of the K^0 production. For reactions (5.1), (5.2), the schematic illustration of the K^0 tagging system is shown in Figure 2. For example, the incoming π^- or K^- defined by the scintillator counter S2 enters a segmented target (ST),

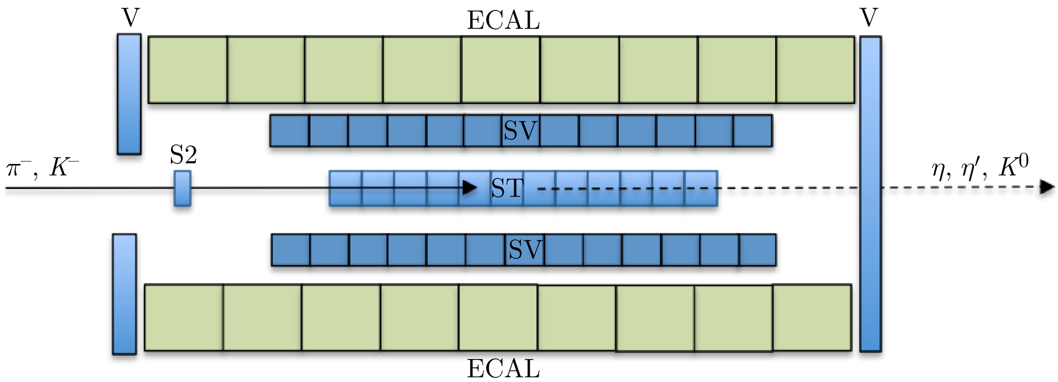

Figure 2. Schematic illustration of the target equipped to search for the invisible decays of neutral kaons in the proposed experiment and tagging the reaction (5.1). The incoming K^- is defined by the counter S; SV is the scintillator veto counter; ECAL is a guard veto electromagnetic calorimeter against the electromagnetic secondaries.

which consists of 12 scintillator cells numbered from $i = 1$ to 12, and produces the leading K^0 accompanied by a low-energy recoil neutron or nuclear fragments.

The occurrence of $K_S, K_L \to invisible$ decays produced in K^- interactions would appear as an event with a signal in the T, see Figure 2 and zero energy deposition in the rest of the detector. Thus, the signal candidate events have the signature

$$S_{K^0 \to invisible} = \mathrm{T} \cdot \overline{\mathrm{SV} \cdot \mathrm{ECAL} \cdot \mathrm{V} \cdot \mathrm{HCAL}} \tag{5.3}$$

and should satisfy the following selection criteria:

(i) The measured momentum of the incoming kaon should correspond to its selected value.

(ii) The kaon should enter the target and the interaction vertex should be localized within the target cell T_j with $1 < j < 12$, with a MIP signal in cells with the number $i < j$, and no signal in cells $i > J$.

(iii) There should be no energy deposition in the ECAL veto, SV and V.

(iv) The fraction of the beam energy deposited in the veto HCAL modules and HCAL should be consistent with zero.

In the case of using reaction (5.2) as the source of K^0's, one can additionally tag them via the presence of the Λ decay products. The segmented SV counters surrounding the target T can be used to detect $\pi^- + p$ pairs from the decay $\Lambda \to \pi^- + p$, while the $\gamma\gamma$ pair from the decay chain $\Lambda \to \pi^0 + n; \pi^0 \to \gamma\gamma$ could be registered in the segmented ECAL calorimeter surrounding the T, as shown in Figure 2. The development of such a tagging system, including possible detection of recoil neutrons from reaction (5.1), is currently under consideration.

5.3. Background and expected sensitivity

The background processes resulting in the signature of the primary reaction (5.1), and similarly of (5.2), can be classified as being due to physical and beam-related sources. To perform a full detector simulation in order to investigate these backgrounds down to the level $\lesssim 10^{-10}$ would require a prohibitively large amount of computer time. Consequently, only the following sources of background — identified as the most dangerous — are considered and evaluated with reasonable statistics combined with numerical calculations:

(i) One of the main background sources is related to the low-energy tail in the distribution of the energy of the primary hadronic beam. This tail is caused by the beam interactions with a passive material, such as the entrance windows of the beam lines, residual gas, etc. Another source of low-energy hadrons is due to beam $\pi^\pm, K^\pm$ decays in flight into a low-energy secondary electron, pions or muons that mimic the signature (5.3) in the detector. For example, the beam π^- or K^- meson could decay into a backward e^- or μ^- with a very low energy, $\lesssim$ 50 MeV, that stops in the target mimicking the charge-exchange signature. To improve the primary high-energy hadron selection and suppress background from the possible admixture of low-energy particles, one can use a tagging system utilizing the magnetic spectrometer installed upstream of the detector, shown in Figure 1, and the K^0 tagging system discussed in Subsection 5.2. Additionally, Cherenkov counters can be used to identify kaons which are expected to be the main source of this background.

(ii) The background events could also arise when the leading K_L or neutron from the reaction $\pi + A \to K_L,\ n + X$ that occurred in the target is not detected due to the incomplete hermeticity of the HCAL. In this case, e.g., the K_L punches through the HCAL without depositing energy above a certain threshold $E_{\rm th}$. The punch-through probability is defined roughly by $\simeq \exp(-L_{\rm HCAL}/\lambda_{\rm int})$, where $L_{\rm HCAL}$ is the HCAL thickness. Thus, by selecting the total HCAL thickness about $28\lambda_{\rm int}$, this background can be suppressed down to the level $\simeq 10^{-12}$.

(iii) Another type of background process is caused by $\pi, K \to \mu, e + \nu$ decays in flight of pions and kaons after they have passed the magnetic spectrometer. The background of the low-energy muon admixture in the beam from the $\pi, K \to \mu\nu$ decays can be due to the following event chain. The decay muon entering the detector decays in flight into a low-energy electron and a neutrino pair, $\mu \to e\nu\nu$ in the target. The electron then penetrates Veto without being efficiently detected, and deposits all its energy in the HCAL, which is below the threshold $E_{\rm th} \lesssim 0.5$ GeV. The probability for this event chain is found to be as small as $P \lesssim 10^{-12}$–10^{-11}. Similar background caused by the decays of the beam pions or kaons in the target was also found to be negligible.

(iv) The fake signature could be due to the physical background: a muon scattering on a nucleon, e.g., $\mu^- p \to \nu_\mu n$, accompanied by a poorly detected neutron. Taking into account the corresponding cross section and the probability for the recoil neutron to escape detection in the HCAL results in an overall level of this background of $\lesssim 10^{-12}$ per incoming hadron.

In Table 1, contributions from all the background processes are summarized for the primary π^- beams with energy 15 GeV. The total background is expected to be at the level $\lesssim 10^{-11}$ per incoming pion. Therefore, the search accumulated up to a few 10^{11} events is expected to be background free. The expected sensitivity in branching fractions is summarized below. assuming the background free search.

To estimate the sensitivity of the proposed experiment, a simplified feasibility study based on GEANT4 [69] Monte Carlo simulations has been performed for 15 GeV pions and kaons. The ECAL is an array of the lead-scintillator counters allowing for accurate measurements of the lateral energy leak from the target. The target is a set of plastic scintillator cells of thickness $\simeq 0.04\lambda_{\rm int}$ viewed by a SiPM photodetector. The SV veto counters are 1–2 cm thick,

Table 1. Expected contributions to the total level of background from different background sources estimated per incident π^- (see text for details).

Source of background	Expected level
HCAL nonhermeticity	$\lesssim 10^{-12}$
Punch-through K^0s	$\sim 10^{-12}$
$\pi^-, K^- \to \mu^-\nu + X$ decays in flight	$\lesssim 10^{-11}$
$\pi^-, K^- \to e^-\nu + X$ decays in flight	$\lesssim 10^{-12}$
μ^- induced reactions on target nuclei	$\lesssim 10^{-12}$
Very low-energy tail of the beam	$\lesssim 10^{-11}$
Total (conservative)	$\lesssim 10^{-11}$ per incoming pion

high-sensitivity Sc arrays with a high light yield of $\simeq 10^3$ photoelectrons per 1 MeV of deposited energy. It is also assumed that the veto's inefficiency for the MIP detection is, conservatively, $\lesssim 10^{-4}$. The hadronic calorimeter is a set of four modules. Each module is a sandwich of alternating layers of iron and scintillator with thicknesses of 25 mm and 4 mm, respectively, and with a lateral size of 60 × 60 cm. Each module consists of 48 such layers and has a total thickness of $\simeq 7\lambda_{\rm int}$. The number of photoelectrons produced by a MIP crossing the module is in the range $\simeq$ 200–300 ph.e. The probability for an event with the MIP energy deposited in the HCAL to mimic the signal due to fluctuations of $n_{\rm ph.e.}$ is negligible. The hadronic energy resolution of the HCAL calorimeters as a function of the beam energy is taken to be $\frac{\sigma}{E} \simeq \frac{60\%}{\sqrt{E}}$ [70]. The energy threshold for the zero energy in the HCAL is 0.1 GeV. The reported further analysis also takes into account passive materials from the DV vessel walls. To estimate the expected sensitivities, we used simulations of the process shown in Figure 1 to calculate fluxes and energy distributions of mesons produced in the target by taking into account the relative normalization of the yield of K^0 from the original publications [71, 72]. For the purpose of this work, the total K^0 production cross sections in the π, K^- charge-exchange reactions in the target were calculated from their extrapolation to the target atomic number as described in [13]. Note that the yield of K^0 is also supposed to be measured *in situ* (see discussion below). Typically, the branching fractions of the charge-exchange reactions are in the range $\frac{\sigma(K^-p\to\overline{K}^0 n)}{\sigma(K^-p\to {\rm all})} \simeq \frac{\sigma(\pi^-p\to\pi^0 n)}{\sigma(\pi^-p\to {\rm all})} \simeq 10^{-4}$–$10^{-3}$ and depend on the beam energy [71, 72].

The calculated fluxes and energy distributions of mesons produced in the target are used to predict the number of signal events in the detector. For a given number of primary pions N_{π^-}, the expected total number of $K_{S,L} \to invisible$ decays occurring within the decay length L of the detector is given by

$$n_K^{\rm inv} = n_{K_S}^{\rm inv} + n_{K_L}^{\rm inv} \tag{5.4}$$

with

$$n_{K_{S,L}}^{\rm inv} = kN_{\pi^-}{\rm Br}\left(K_{S,L} \to invisible\right) \cdot \int \frac{\sigma(\pi^- + A \to K^0 + \ldots)}{dt} \times \\ \times \left[1 - \exp\left(-\frac{LM_{K^0}}{P_{K^0}\tau_{K_{S,L}}}\right)\right] \zeta\epsilon_{\rm tag}\, dt \simeq \zeta\epsilon_{\rm tag}{\rm Br}\left(K_{S,L} \to invisible\right) n_{K_{S,L}}^{\rm dec}, \tag{5.5}$$

where the coefficient k is a normalization factor that was tuned to obtain the total cross section of the meson production; P_{K^0} and τ_{K^0} are the K^0 momentum and the lifetime of either K_S or K_L at rest, respectively; ζ is the signal reconstruction efficiency; $\epsilon_{\rm tag}$ is the tagging efficiency of the final state; and $n_{K_{S,L}}^{\rm dec}$ is the total number of $K_{S,L}$ decays occurring in the decay volume of length L. In this estimate we neglect the K^0 interactions in the target: the average momentum of the incoming kaons is in the range $\langle p_{K^-}\rangle \simeq 15$ GeV, the decay length is $L \simeq 5$ m, and the efficiency is $\zeta \simeq 0.9$. The tagging efficiency $\epsilon_{\rm tag}$ is typically $\gtrsim 90\%$ [71–73].

In the case of no signal observation, the obtained results can be used to impose upper limits on the decays of $K_{S,L}$ into invisible final states; by using the relation $n_K^{\rm inv} = n_{K_S}^{\rm inv} + n_{K_L}^{\rm inv} < n_{90\%}^{\rm inv}$, where $n_{90\%}^{\rm inv}$ (= 2.3 events) is the 90% C.L. upper limit for the number of signal events, and Eq. (5.5), one can determine the expected 90% C.L. upper limits from the results of the proposed experiment summarized in Table 2 for the total number of $3 \cdot 10^{10}$ pions on target. Here we also assume that the exposure to the π/K beam with the nominal rate is a few months and that the invisible final states do not decay promptly into the ordinary particles, which would deposit energy in the veto system or HCAL.

Table 2. Expected upper limits on the branching ratios of different decays into invisible final states calculated for the total number of $3 \cdot 10^{11}$ incident pions and reaction (5.2) as the source of $K_{S,L}$ (see text for details).

Expected limits	Present limit
$\mathrm{Br}\,(K_S \to \mathit{invisible}) \lesssim 10^{-7}$	No
$\mathrm{Br}\,(K_L \to \mathit{invisible}) \lesssim 10^{-5}$	No
$\mathrm{Br}\,(\eta \to \mathit{invisible}) \lesssim 2.7 \cdot 10^{-7}$	$< 1.0 \cdot 10^{-4}$ [17, 18]
$\mathrm{Br}\,(\eta' \to \mathit{invisible}) \lesssim 5.6 \cdot 10^{-7}$	$< 2.1 \cdot 10^{-4}$ [18]

By taking Eqs. (4.12), (4.13) into account, the expected limits of Table 2 can be transformed in the bound on the probability of the K_L–K_L^M oscillation and the mixing strength δ. For numerical estimates, we shall take the energy of kaons equal to $E_K = 15$ GeV and the decay length of the detector for K_S, K_L decays equal to $L_0 = 5$ m. For K_S mesons with the energy E_0, the decay length is $l_{K_S} = c\tau_{K_S} \cdot \frac{E_K}{m_K} = 0.8$ m $\ll L_0$. Here $c = 3 \cdot 10^8$ m/s is the velocity of light. It means that we can use formula (4.13) for the estimate of the transition probability $P(K_S \to K_S^M)$ of the K_S meson into the dark K_S meson. Taking the bound on the invisible K_S decay, $\mathrm{Br}\,(K_S \to \mathit{invisible}) = 10^{-7}$ and using Eq. (4.13), we can obtain the bound

$$\frac{\delta_{K_S}}{\Gamma_{K_S}} \leqslant 4.5 \cdot 10^{-4}. \tag{5.6}$$

For K_L mesons the situation is different. Indeed, for K_L mesons the decay length is $l_{K_L} = c\tau_{K_L} * \frac{E_K}{m_K} = 466\ m \gg L_0$. It means that only a small fraction of the produced K_L's decay inside the detector. As a consequence, Eq. (4.8) takes the form

$$P_{\rm int}(K_L \to K_L^M | t \leqslant t_0) \approx \frac{m_K^2}{12E_K^2}\delta^2 t_0^3, \tag{5.7}$$

where $t_0 \approx \frac{L_0}{c}$. The use of formula (5.7) gives

$$P_{\rm rel}(K_L \to K_L^M) \approx \frac{m_K^2}{12E_K^2}\delta^2 t_0^2, \tag{5.8}$$

Taking the bound $\mathrm{Br}\,(K_L \to \mathit{invisible}) = 10^{-5}$ from Table 2 and Eq. (5.8) into account, one can obtain for K_L the bound

$$\frac{\delta_{K_L}}{\Gamma_{K_L}} \leqslant 1, \tag{5.9}$$

which is, as discussed above, rather weak due to the fact that the fraction of K_L's decaying at the length $0 \leqslant l \leqslant 5\ m$ is just $1 - \exp\left(-\Gamma_{K_L} \frac{m}{E_K} t_0\right) = 0.01$. However, due to the fact that $\Gamma_{K_L} \ll \Gamma_{K_S}$, the expected limits for δ_{K_L} and δ_{K_S} don't differ strongly, namely,

$$\begin{aligned} \delta_{K_L} &\leqslant 1.3 \cdot 10^{-17}\ \text{GeV}, \\ \delta_{K_S} &\leqslant 0.33 \cdot 10^{-17}\ \text{GeV}. \end{aligned} \tag{5.10}$$

In the case of a signal observation, several methods could be used to cross-check the result. For instance, to test whether the signal is due to the HCAL non-hermeticity or not, one could perform measurements with different HCAL thicknesses, i.e., with one, two, three, and four consecutive HCAL modules. In this case, the expected background level could be obtained by extrapolating the results to an infinite HCAL thickness. The evaluation of the signal and background could also be obtained from the results of measurements at different beam energies.

The signal from $K_{S,L}$–$K_{S,L}^M$ oscillations can be cross-checked by

- modifying the length of the K^0 decay volume,
- changing the air pressure in the decay volume,
- changing the energy of the beam.

6. Conclusion

Due to their specific properties, neutral kaons are one of the most interesting probes of physics beyond the Standard Model from both theoretical and experimental viewpoints. The decays $K_{S,L} \to$ *invisible* have never been experimentally tested. In the Standard Model their branching ratios for the decay into two neutrinos are predicted to be extremely small, $\text{Br}\,(K_{S,L} \to \nu\bar{\nu}), \lesssim 10^{-16}$. Thus, observation of $K_{S,L} \to$ *invisible* decays would unambiguously signal the presence of new physics.

We consider the $K_L \to$ *invisible* decay in several natural extensions of the SM, such as the 2HDM, 2HDM and light neutral scalar field ϕ, and dark mirror matter model. Using constraints from the experimental value for the $\text{Br}\,(K^+ \to \pi^+\nu\bar{\nu})$, we find that the $K_{S,L} \to$ *invisible* decay branching ratio could be in the region $\text{Br}\,(K_{S,L} \to invisible) \simeq 10^{-8}$–$10^{-6}$, which is experimentally accessible, allowing one to test new-physics scales well above 100 TeV. In some scenarios, the bound $\text{Br}\,(K_{S,L} \to \nu\bar{\nu}) \lesssim 10^{-16}$ can be avoided, as in the model with the massive right-handed neutrino and scalar ϕ particle. All this makes these decays a powerful clean probe of new physics, which is complementary to other rare K-decay channels. Additionally, in the case of observation, $K_{S,L} \to$ *invisible* decays could influence the Bell–Steinberger analysis of the K^0–$\overline{K}^0$ system.

The results obtained provide a strong motivation for a sensitive search for these decay modes in a near future experiment similar to the one proposed in [4]. We briefly discussed such a search with the pion and kaon beams available at the CERN PS and SPS, which would also be capable of improving sensitivity for invisible decays of η, η' and other neutral mesons. If such decays exist, they could be observed by looking for events with a striking signature: the total disappearance of the beam energy in a fully hermetic hadronic calorimeter. A feasibility study of the experimental setup shows that this unique signature allows for searches of $K_S, K_L \to$ *invisible* decays with a sensitivity in the branching ratio $\text{Br}\,(K_{S,L} \to invisible) \lesssim 10^{-7}$–$10^{-5}$, and $\eta, \eta' \to$ *invisible* decays with a sensitivity a few orders of magnitude beyond the present experimental limits.

These results could be obtained with a detector that is optimized for several of properties; namely, i) the intensity and purity of the primary pion and kaon beams, ii) high-efficiency tagging of the K^0 production, and iii) a high level of hermeticity in the hadronic calorimeter system are of importance. Large amounts of high-energy hadrons and high background suppression are crucial to improving the sensitivity of the search. To obtain the best limits, a compromise should be found between the background level and the energy and intensity of the beam.

Finally, we note that the presented analysis gives an illustrative order of magnitude for the sensitivity of the proposed experiment and may be strengthened by more detailed simulations of the experimental setup.

Acknowledgments

We would like to thank our colleagues from the NA64 collaboration for their interest in this work. In particular, we are grateful to L. Molina Bueno, A. Celentano, P. Crivelli, S. Donskov, M. Kirsanov, S. Kuleshov, V. Lyubovitskij, D. Peshekhonov, V. Poliakov, V. Samoylenko, A. Toropin, and A. Zevlakov for useful discussions.

Conflict of Interest

The authors declare no conflict of interest.

References

[1] R. L. Workman et al. (Particle Data Group), Progress of Theoretical and Experimental Physics 2022 (2022) 083C01.

[2] L. Gan, B. Kubis, E. Passemar, and S. Tulin, Physics Reports 945 (2022) 1.

[3] J. F. Kamenik and C. Smith, Journal of High Energy Physics 03 (2012) 090.

[4] S. N. Gninenko, Physical Review D 91 (2015) 015004.

[5] S. N. Gninenko and N. V. Krasnikov, Physical Review D 92 (2015) 034009.

[6] S. N. Gninenko and N. V. Krasnikov, Modern Physics Letters A 31 (2016) 1650142.

[7] D. Barducci, M. Fabbrichesi, and E. Gabrielli, Physical Review D 98 (2018) 035049.

[8] M. Hostert, K. Kaneta, and M. Pospelov, Physical Review D 102 (2020) 055016.

[9] J. Elam et al. (REDTOP Collaboration), arXiv:2203.07651.

[10] P. Schuster, N. Toro, and K. Zhou, Physical Review D 105 (2022) 035036.

[11] A. S. Zhevlakov, D. V. Kirpichnikov, S. N. Gninenko, S. V. Kuleshov, and V. E. Lyubovitskij, Physical Review D 108 (2023) 115005.

[12] S. N. Gninenko, D. V. Kirpichnikov, S. V. Kuleshov, V. E. Lyubovitskij, and A. S. Zhevlakov, arXiv: 2407.01181.

[13] S. N. Gninenko, D. V. Kirpichnikov, S. V. Kuleshov, V. E. Lyubovitskij, and A. S. Zhevlakov, Physical Review D 109 (2024) 075021.

[14] I. V. Voronchikhin, D. V. Kirpichnikov, Physical Review D 107 (2023) 115034; Physical Review D 106 (2022) 115041. arXiv: 2409.12748.

[15] A. V. Artamonov et al. (E949 Collaboration), Physical Review D 72 (2005) 091102.

[16] E. Cortina Gil et al. (NA62 Collaboration), Journal of High Energy Physics 05 (2019) 182.

[17] M. Ablikim et al. (BES Collaboration), Physical Review 87 (2013) 012009.

[18] Yu. M. Andreev et al. (NA64 Collaboration), Physical Review Letters 133 (2024) 121803.

[19] C. L. Hsu et al. (Belle Collaboration), Physical Review D 86 (2012) 032002.

[20] B. Aubert et al. (BaBar Collaboration), Physical Review Letters 93 (2004) 091802.

[21] M. Ablikim et al. (BES Collaboration), Physical Review Letters 100 (2008) 192001.

[22] P. Rubin et al. (CLEO Collaboration), Physical Review D 75 (2007) 031104.
[23] S. N. Ahmed et al. (SNO Collaboration), Physical Review Letters 92 (2004) 102004.
[24] H. O. Back et al. (Borexino Collaboration), Physics Letters B 563 (2003) 23.
[25] T. Araki et al., Physical Review Letters 96 (2006) 101802.
[26] V. I. Tretyak, V. Yu. Denisov, and Yu. G. Zdesenko, Journal of Experimental and Theoretical Physics Letters 79 (2004) 106; Pis'ma v Zhurnal Eksperimentalnoi i Teoreticheskoi Fiziki 79 (2004) 136. nucl-ex/0401022.
[27] H. V. Klapdor-Kleingrothaus, I. V. Krivosheina, and I. V. Titkova, Physics Letters B 644 (2007) 109.
[28] G. Banet et al., Physical Review Letters 99 (2007) 161603.
[29] N. J. Ayres et al., Symmetry 14 (2022) 503.
[30] A. P. Serebrov et al., Physics Letters B 663 (2008) 181.
[31] M. Sarrazin, G. Pignol, F. Petit, and V. V. Nesvizhevsky, Physics Letters B 712 (2012) 213.
[32] S. N. Gninenko, N. V. Krasnikov, and A. Rubbia, Physical Review D 67 (2003) 075012.
[33] A. Badertscher, P. Crivelli, U. Gendotti, S. N. Gninenko, V. Postoev, A. Rubbia, V. Samoylenko, and D. Sillou, Physical Review D 75 (2007) 032004.
[34] P. Crivelli, A. Belov, U. Gendotti, S. Gninenko, and A. Rubbia, Journal of Instrumentation 5 (2010) P08001. arXiv:1005.4802 [hep-ex];
C. Vigo et al., Physical Review D 97 (2018) 092008; Physical Review Letters 124 (2020) 101803.
[35] S. N. Gninenko, N. V. Krasnikov, and V. A. Matveev, Physical Review D 87 (2013) 015016. arXiv:1209.0060 [hep-ph].
[36] S. N. Gninenko, Physical Review D 76 (2007) 055004.
[37] W. J. Marciano and Z. Parsa, Physical Review D 53 (1996) R1.
[38] D.-N. Gao, Physical Review D 98 (2018) 113006.
[39] A. J. Buras and J. Girrbach, Reports on Progress in Physics 77 (2014) 086201.
[40] V. Cirigliano, G. Ecker, H. Neufeld, A. Pich, and J. Portoles, Reviews of Modern Physics 84 (2012) 399.
[41] D. Bryman, W. J. Marciano, R. Tschirhart, and T. Yamanaka, Annual Review of Nuclear and Particle Science 61 (2011) 331.
[42] T. K. Komatsubara, Progress in Particle and Nuclear Physics 67 (2012) 995.
[43] M. Blanke, arXiv:1305.5671(2013).
[44] L. G. Landsberg, Physics–Uspekhi 46 (2003) 995; Uspekhi Fizicheskikh Nauk 46 (2003) 1025.
[45] J. S. Bell and J. Steinberger, in: Oxford International Symposium Conference on Elementary Particles, Oxford, England, September 19–25, 1965, edited by L. Wolfenstein, Rutherford High Energy Laboratory, Chilton, 1965, p. 42.
[46] J. Steinberger, K^0 Decay and CP Violation, CERN 70-1, 1970.
[47] M. Antonelli, G. D'Ambrosio, and M. S. Sozzi, CPT Invariance Tests in Neutral Kaon Decay, p. 871, in Ref. [1].
[48] L. Maiani, in: The Second DAPHNE Physics Handbook, two volumes, edited by L. Maiani, G. Pancheri, and N. Paver, INFN, Frascati, 1995, 1202 p.
[49] G. D'Ambrosio, G. Isidori, and A. Pugliese, in: The Second DAPHNE Physics Handbook, two volumes, edited by L. Maiani, G. Pancheri, and N. Paver, INFN, Frascati, 1995, 1202 p.
[50] P. Bloch and L. Tauscher, Annual Review of Nuclear and Particle Science 53 (2003) 123.
[51] F. Ambrosino et al. (KLOE Collaboration), Journal of High Energy Physics 0612 (2006) 011. arXiv:hep-ex/0610034.
[52] A. Angelopoulosetal et al. (CPLEAR Collaboration), Physics Letters B 471 (1999) 332.
[53] K. R. Schubert, L. Li Gioi, A. J. Bevan, and A. Di Domenico, arXiv:1401.6938 [hep-ex].
[54] J. N. Butler et al., arXiv:1311.1076(2013).

[55] V. Rubakov and D. Gorbunov, Introduction to the Theory of the Early Universe, 1st Edition, World Scientific Publishing Co., Singapore, 2017.

[56] E. W. Kolb and M. S. Turner, The Early Universe, FERMILAB-BOOK-1990-01, 1990.

[57] T. D. Lee and C. N. Yang, Physical Review 104 (1956) 254;
I. Kobzarev, L. Okun, and I. Pomeranchuk, Soviet Journal of Nuclear Physics 3 (1966) 837.

[58] S. I. Blinnikov and M. Yu. Khlopov, Soviet Journal of Nuclear Physics 36 (1982) 472; Soviet Astronomy AJ 27 (1982) 371;
R. Foot, H. Lew, and R. R. Volkas, Physics Letters B 272 (1991) 67;
Z. Berezhiani and R. Mohapatra, Physical Review D 62 (1995) 6607;
L. B. Okun, Physics–Uspekhi 50 (2007) 380; Uspekhi Fizicheskikh Nauk 177 (2007) 397.

[59] R. Foot, International Journal of Modern Physics A 29 (2014) 1430013.

[60] A. Yu. Ignatiev and R. R. Volkas, Physics Letters B 487 (2000) 294;
B. Patt and F. Wilczek, arXiv: hep-ph/0605188.

[61] S. L. Glashow, Physics Letters B 167 (1986) 35;
S. N. Gninenko, Physics Letters B 326 (1994) 317;
R. Foot and S. N. Gninenko, Physics Letters B 480 (2000) 171.

[62] Z. Berezhiani and L. Bento, Physical Review Letters 96 (2006) 081801;
Z. Berezhiani, European Physical Journal C 64 (2009) 421.

[63] N. N. Nikolaev and L. B. Okun, Physics Letters 27B (1968) 226.

[64] S. N. Gninenko, N. V. Krasnikov, and V. A. Matveev, Physics of Particles and Nuclei 51 (2020) 829.

[65] S. N. Gninenko, N. V. Krasnikov, and V. A. Matveev, Uspekhi Fizicheskikh Nauk 191 (2021) 1361.

[66] S. N. Gninenko, Physical Review D 89 (2014) 075008. arXiv:1308.6521 [hep-ph].

[67] S. Andreas et al., arXiv:1312.3309 [hep-ex], CERN-SPSC-2013-034/SPSC-P-348.

[68] http://sba.web.cern.ch/sba/.

[69] S. Agostinelli et al. (GEANT4 Collaboration), Nuclear Instruments and Methods in Physics Research, Section A 506 (2003) 250;
J. Allison et al. (GEANT4 Collaboration), IEEE Transactions on Nuclear Science 53 (2006) 270.

[70] G. A. Alekseev et al., Nuclear Instruments and Methods in Physics Research, Section A 461 (2001) 381.

[71] F. Binon et al., Il Nuovo Cimento A 64 (1981) 89.

[72] V. N. Bolotov et al., Nuclear Physics B 85 (1975) 158.

[73] F. Binon et al., Zeitschrift für Physik C 9 (1981) 109.